ISSN 1674-1056
http://cpb.iphy.ac.cn
http://iopscience.iop.org/cpb
中国物理 B
Chinese Physics
中国物理 Chinese Physics B

Tunneling magnetoresistance in ferromagnet/organic-ferromagnet/metal junctions

Yan-Qi Li(李彦琪), Hong-Jun Kan(阚洪君), Yuan-Yuan Miao(苗圆圆), Lei Yang(杨磊), Shuai Qiu(邱帅), Guang-Ping Zhang(张广平), Jun-Feng Ren(任俊峰), Chuan-Kui Wang(王传奎), Gui-Chao Hu(胡贵超)

Citation: Chin. Phys. B . 2020, 29(1): 017303 . **doi:** 10.1088/1674-1056/ab5d02
Journal homepage: http://cpb.iphy.ac.cn; http://iopscience.iop.org/cpb

What follows is a list of articles you may be interested in

Effects of oxygen vacancy concentration and temperature on memristive behavior of $SrRuO_3$/Nb:$SrTiO_3$junctions

Zhi-Cheng Wang(王志成), Zhang-Zhang Cui(崔璋璋), Hui Xu(徐珲), Xiao-Fang Zhai(翟晓芳), Ya-Lin Lu(陆亚林)\
Chin. Phys. B . 2019, 28(8): 087303 . **doi:** 10.1088/1674-1056/28/8/087303

Spin-valley-dependent transport and giant tunneling magnetoresistance in silicene with periodic electromagnetic modulations

Yi-Man Liu(刘一曼), Huai-Hua Shao(邵怀华), Guang-Hui Zhou(周光辉), Hong-Guang Piao(朴红光), Li-Qing Pan(潘礼庆), Min Liu(刘敏)
Chin. Phys. B . 2017, 26(12): 127303 . **doi:** 10.1088/1674-1056/26/12/127303

Length dependence of rectification in organic co-oligomer spin rectifiers

Gui-Chao Hu(胡贵超), Zhao Zhang(张朝), Ying Li(李营), Jun-Feng Ren(任俊峰), Chuan-Kui Wang(王传奎)
Chin. Phys. B . 2016, 25(5): 057308 . **doi:** 10.1088/1674-1056/25/5/057308

Effect of interfacial coupling on rectification in organic spin rectifiers

Hu Gui-Chao, Zuo Meng-Ying, Li Ying, Zhang Zhao, Ren Jun-Feng, Wang Chuan-Kui
Chin. Phys. B . 2015, 24(7): 077308 . **doi:** 10.1088/1674-1056/24/7/077308

Spin-excited states and rectification in an organic spin rectifier

Zuo Meng-Ying, Hu Gui-Chao, Li Ying, Ren Jun-Feng, Wang Chuan-Kui
Chin. Phys. B . 2014, 23(8): 087306 . **doi:** 10.1088/1674-1056/23/8/087306

Tunneling magnetoresistance in ferromagnet/organic-ferromagnet/metal junctions*

Yan-Qi Li(李彦琪)†, Hong-Jun Kan(阚洪君)†, Yuan-Yuan Miao(苗圆圆), Lei Yang(杨磊), Shuai Qiu(邱帅), Guang-Ping Zhang(张广平), Jun-Feng Ren(任俊峰), Chuan-Kui Wang(王传奎), and Gui-Chao Hu(胡贵超)‡

Shandong Province Key Laboratory of Medical Physics and Image Processing Technology, School of Physics and Electronics, Shandong Normal University, Jinan 250100, *China*

(Received 3 October 2019; revised manuscript received 13 November 2019; accepted manuscript online 29 November 2019)

Spin-dependent transport in ferromagnet/organic-ferromagnet/metal junctions is investigated theoretically. The results reveal a large tunneling magnetoresistance up to 3230% by controlling the relative magnetization orientation between the ferromagnet and the central organic ferromagnet. The mechanism is explained by distinct efficient spin-resolved tunneling states in the ferromagnet between the parallel and antiparallel spin configurations. The key role of the organic ferromagnet in generating the large magnetoresistance is explored, where the spin selection effect is found to enlarge the difference of the tunneling states between the parallel and antiparallel configurations by comparing with the conventional organic spin valves. The effects of intrinsic interactions in the organic ferromagnet including electron–lattice interaction and spin coupling with radicals on the magnetoresistance are discussed. This work demonstrates a promising potential of organic ferromagnets in the design of high-performance organic spin valves.

Keywords: organic ferromagnet, organic spintronics, tunneling magnetoresistance

PACS: 73.63.–b, 75.47.–m, 85.75.–d **DOI:** 10.1088/1674-1056/ab5d02

1. Introduction

Spin valves, in which a nonmagnetic layer is usually sandwiched between two ferromagnetic electrodes, play an important role in the field of spintronics for information storage and developing spin transfer and spin orbit torque spintronic devices.[1–5] Recently, the utilization of organic molecules as the central layers has attracted much attention.[6–13] It not only rouses the prospect of low-cost and flexible devices, but also brings many physical merits to spin transport compared with the inorganic counterpart, such as the long spin relaxation time induced by the weak spin–orbit and hyperfine interactions,[14] and the tunable interfacial spin polarization caused by the orbital hybridization at the organic/inorganic interfaces.[15–19] The exploration of novel organic materials for high-performance spintronic devices keeps an intriguing issue in the field of organic spintronics.

Organic ferromagnets (OFs) are fascinating since they combine both the ferromagnetic and organic properties. Organic magnets may be fabricated by doping transition ions into organic components, such as V[TCNE]$_x$ (TCNE = tetracyanoethylene),[20] or using spin radicals, such as poly-BIPO (poly-(1,4-bis(2,2,6,6-tetramethyl-4-piperidyl-1-oxyl)-butadiin).[21,22] In the last years, OFs have triggered more and more interests in experiments to seek novel property in organic spin valves. Yoo *et al.* used V[TCNE]$_x$ as the spin injector and measured the magnetoresistance (MR) in V[TCNE]$_x$/rubrene/LSMO junctions, where a MR up to 6% was obtained.[23] A small MR at room temperature was reported with V[TCNE]$_x$ as the central layers.[24] Hayakawa *et al.* experimentally demonstrated that in the presence of a spin radical, the tunneling magnetoresistance (TMR) was enhanced by one order of magnitude.[25] Several theoretical designs of spintronic devices based on OFs were also involved including spin-filtering[26–28] and multi-state MR.[29]

In spite of that, still little is known about the TMR in OF based spin valves, especially the underlying unique role of the OF compared with the conventional organic spin valves. Due to the intrinsic magnetism of the OF, only one ferromagnet is required for the construction of the spin valve, which is different from the conventional organic spin valves with two ferromagnets. The TMR property in such structure is seldom involved in the past studies and the comparison with conventional organic spin valves is necessary. In this paper, we construct an OF spin valve by connecting the OF with one ferromagnetic and one nonmagnetic electrodes. By calculating the spin-dependent transport, an extremely high TMR up to 3230% is demonstrated. A comparison with conventional organic spin valves is performed, where the crucial role of the OF in enlarging the difference of the efficient tunneling states between parallel (P) and antiparallel (AP) configurations is analyzed. The paper is organized as follows: the model and calculation method are introduced in Section 2. In Section 3, the

*Project supported by the National Natural Science Foundation of China (Grant Nos. 11974215, 11704230, 11674197, and 11874242), the Natural Science Foundation of Shandong Province, China (Grant No. ZR2019MA043), and the Taishan Scholar Project of Shandong Province, China.

†These two authors contributed equally to this work.

‡Corresponding author. E-mail: hgc@sdnu.edu.cn

© 2020 Chinese Physical Society and IOP Publishing Ltd

numerical results and physical analysis are presented. At last, a summary is given in Section 4.

2. Model and calculation method

Schematic of the device model is shown in Fig. 1. Here an OF molecule with spin radicals is connected with one ferromagnet and one normal metal. The two electrodes are modeled as one-dimensional semi-infinite chains. The typical OF molecule poly-BIPO is adopted, which has a quasi-one-dimensional structure composed of the main chain and spin radicals on the odd-number sites. At ground state, the radical spins will form a ferromagnetic order.[30] Such model is also valid for other OFs with different spin radicals.[31] The OF can be described by the extended Su–Schrieffer–Heeger (SSH) model combined with a Kondo term[21,22,29,30,32]

$$\begin{aligned} H_{\rm OF} =& \sum_{i,\sigma}\left[\varepsilon_0 c^+_{i,\sigma}c_{i,\sigma} - t_i\left(c^+_{i,\sigma}c_{i+1,\sigma}+{\rm H.c.}\right)\right] \\ &+U\sum_i c^+_{i,\uparrow}c_{i,\uparrow}c^+_{i,\downarrow}c_{i,\downarrow}+W\sum_{i,\sigma,\sigma'}c^+_{i,\sigma}c_{i,\sigma}c^+_{i+1,\sigma'}c_{i+1,\sigma'} \\ &+J\sum_i \delta_{i,\rm o}\boldsymbol{s}_i\cdot\boldsymbol{S}_{i\rm R}+\frac{K}{2}\sum_i y_i^2. \end{aligned} \tag{1}$$

The first term embodies the energy of itinerant electrons in the main chain. ε_0 is the on-site energy, and $c^+_{i,\sigma}$ ($c_{i,\sigma}$) is the creation (annihilation) operator of an electron with spin σ on site i. $t_i = t_0 - \alpha y_i$ denotes the nearest hopping integral of electrons, where t_0 is the electron transfer integral in a uniform chain and $y_i = (u_{i+1} - u_i)$ is the bond distortion with u_i the displacement of the i-th atom. α stands for the electron–lattice coupling constant. The second and the third terms describe the electron–electron interactions given by an extended Hubbard model[33] with U the on-site interaction and W the site–site one. The fourth term is the antiferromagnetic coupling between the π-electron spin $\boldsymbol{s}_i$ and radical spin $\boldsymbol{S}_{i\rm R}$ with coupling strength J. $\delta_{i,\rm o}$ means the antiferromagnetic coupling only exists at the odd sites. The last term is the lattice elastic energy with elastic coefficient K.

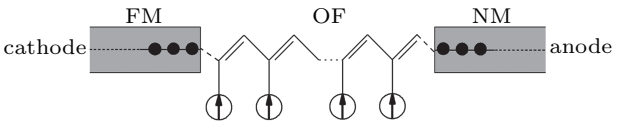


Fig. 1. The schematic of ferromagnet/organic-ferromagnet/metal molecular junctions.

The electrodes are described by the single-band tight-binding model with the Hamiltonian

$$\begin{aligned} H_{\rm L(R)} =& \sum_{i,\sigma}\left[\varepsilon_{\rm l(r)}a^+_{i,\sigma}a_{i,\sigma} - t_{\rm l(r)}\left(a^+_{i+1,\sigma}a_{i,\sigma}+{\rm H.c.}\right)\right] \\ &-\sum_i J_{\rm l(r)}\left(a^+_{i,\uparrow}a_{i,\uparrow}-a^+_{i,\downarrow}a_{i,\downarrow}\right), \end{aligned} \tag{2}$$

where $\varepsilon_{\rm l(r)}$ and $t_{\rm l(r)}$ are the on-site energy and hopping integral of electrons in the left (right) electrode, respectively, $a^+_{i,\sigma}$ ($a_{i,\sigma}$) denotes the creation (annihilation) operator, and $J_{\rm l(r)}$ is a Stoner-like spin splitting constant of the electrode,[34] which naturally vanishes for the right nonmagnetic electrode. The interfacial interaction between the molecule and the electrodes is simplified as a hopping integral ($t_{\rm me}$) between the neighbor sites.

Under a bias, an electric field E is assumed to generate along the molecular chain with the Hamiltonian

$$\begin{aligned} H_E =& -\sum_{i,\sigma}|e|E\left[\left(i-\frac{N+1}{2}\right)a+u_i\right]c^+_{i,\sigma}c_{i,\sigma} \\ &+\sum_i|e|E\left[\left(i-\frac{N+1}{2}\right)a+u_i\right]. \end{aligned} \tag{3}$$

Here e is the electron charge, a the lattice constant, and N the number of total sites in the molecular chain. The first and second terms represent the potential energies of electrons and the lattice ions with one unit of positive charge at each site, respectively. The electric field is related to the bias by $E = V/(N-1)a$. This model is more convenient than solving the Poisson equation when the bias is not too large.[35]

The stable state of the OF under the electric field is obtained by solving the electronic eigen equation and lattice configuration equation self-consistently.[22,26] After that, the spin-resolved current is calculated by Landauer–Büttiker formula[36]

$$I_\sigma(V) = \frac{e}{h}\int_{-\infty}^{+\infty} T_\sigma(E,V)\left[f(E-\mu_{\rm l})-f(E-\mu_{\rm r})\right]{\rm d}E. \tag{4}$$

Here h is the Planck constant,

$$T_\sigma(E,V) = {\rm Tr}\left[\Gamma_{\rm L}G_\sigma(E,V)\Gamma_{\rm R}G^+_\sigma(E,V)\right]$$

is the spin-resolved electronic transmission, and $G_\sigma(E,V)$ is the single-electron retard Green's function for the central molecule. $\Gamma_{\rm L(R)}$ denotes the broadening matrix induced by coupling with the electrodes. $f\left(E-\mu_{\rm l(r)}\right)$ is the Fermi–Dirac distribution function with chemical potential $\mu_{\rm l(r)} = E_{\rm F} \pm eV/2$ and Fermi level $E_{\rm F}$. The charge current is the sum of the spin-resolved currents, $I_{\rm C} = I_\uparrow + I_\downarrow$.

The calculation parameters are chosen as follows. For the OF, we determine the parameters according to the well established values for poly-BIPO,[37,38] $t_0 = 2.5$ eV, $\varepsilon_0 = -6.6$ eV, $\alpha = 4.1$ eV/Å, $K = 21.0$ eV/Å^2, $U = 3W = 1.0$ eV, and $j = J/t_0 = 0.5$. The total site number is $N = 20$. For the electrodes, $\varepsilon_{\rm l} = -6.56$ eV, $\varepsilon_{\rm r} = -5.0$ eV $t_{\rm l} = t_{\rm r} = 1.5$ eV, $J_{\rm l} = 1.5$ eV, and $J_{\rm r} = 0$. The Fermi energy of the two electrodes is chosen as $E_{\rm F} = -5.0$ eV. These parameters are chosen to fit the band structures of Co and Au.[29,39] The interfacial coupling parameter is taken as $t_{\rm me} = 1.0$ eV.

3. Results and discussion

In the present device, the coercive fields of the left ferromagnetic electrode and the central OF molecule are different, e.g., 150 Oe for Co and 295–470 Oe for poly-BIPO.[6,40] Thus the P and AP alignments of the magnetization orientations are expected to be realized by an external magnetic field under the condition of a weak magnetic exchange. In our model, for simplicity, the spins of the radicals in the OF are fixed as up, while the magnetization of the ferromagnet is changeable as up or down. We start our calculations from the currents in the two spin configurations, and the results are shown in Fig. 2(a). Due to the asymmetric structure, both the positive and negative biases are investigated. Obviously, nonlinear current–voltage curves are observed in the two cases, which depend on both the polarity of the bias and the spin configurations. Under positive bias, the threshold voltage in P configuration is about 0.5 V, and the current reaches 2.7 μA at 1.0 V. The threshold voltage in AP configuration is a little larger (∼ 0.6 V), while the current at 1.0 V is only 1.4 μA. Under negative bias, the situation is similar where the AP configuration corresponds to a larger threshold voltage (−0.9 V) and a smaller current (−0.9 μA at −1.0 V) compared to the P configuration (−0.5 V and −3.7 μA at −1.0 V).

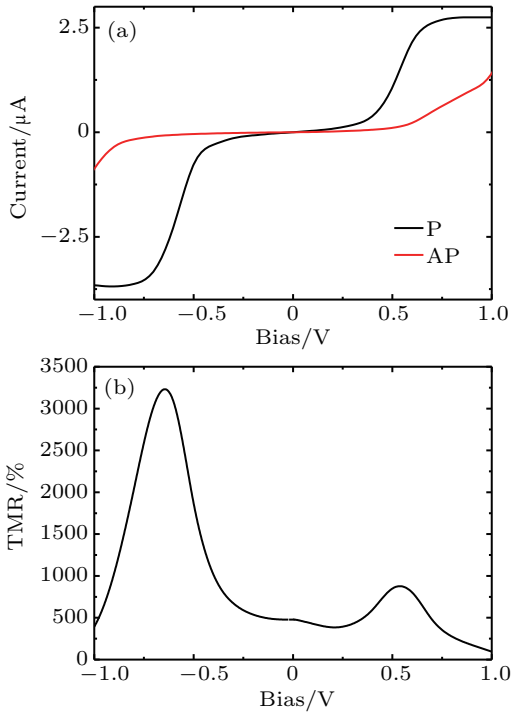


Fig. 2. (a) The charge current with bias in P and AP spin configurations of the Co/OF/Au junction. (b) The TMR of the device versus bias.

In Fig. 2(b), the bias-dependent TMR is displayed, which is defined as $\mathrm{TMR}(V) = [I_{\mathrm{P}}(V) - I_{\mathrm{AP}}(V)]/I_{\mathrm{AP}}(V)$. Positive TMR is obtained in the calculated bias region, where two distinct peaks appear at the two polarities of the bias, respectively. One locates at about 0.54 V with the magnitude of about 887%, and the other lies at −0.64 V with an extremely high value of 3230%. Even the minimum value at 1.0 V is around 100%. This result indicates that a high-performance organic spin valve is realized with the utilization of the OF.

To understand the two high TMR peaks at different polarities of the bias, we first give a sight on the spin-dependent transmission spectra. Figure 3 shows the transmission spectra at 0.6 V and −0.6 V, which are around the TMR peaks and convenient to make a comparison between positive and negative biases. At the positive bias of 0.6 V, the current is contributed by a spin-down peak, which is from the spin-down lowest unoccupied molecular orbital (LUMO) by examining the molecular eigen levels. The height of the peak in P configuration is much higher than that in AP configuration, which is responsible for the current difference as well as the large TMR. At the negative bias of −0.6 V, this spin-down peak in P configuration becomes a little higher, but it turns invisible in AP configuration. Thus, the TMR is further enhanced compared with that at 0.6 V.

The above different transport behaviors can be further understood based on a simple band tunneling sketch. As shown in Fig. 4, the left spin-split Co electrode consists of a full-filled majority band and a half-filled minority one, while the right Au electrode is spin degenerate and half-filled. With the present parameters, the spin-down LUMO of the central OF is close to the Fermi level. Thus, at low bias only spin-down electrons are permitted to transport through the molecule when neglecting the spin flipping process. By applying a positive bias of 0.6 V, the left Co band is lifted and the right Au band is lowered. In P configuration, the spin-down (minority) electrons from the Co electrode tunnel into the right spin-down band of Au via the central spin-down LUMO. In AP configuration, the transmission is contributed by the electron tunneling from the left full-filled majority band to the right half-filled one with down spin. The main difference between the P and AP cases is the involved tunneling states of Co, which stem from the middle of the band in P configuration, while the band-edge states serve in AP configuration. By assuming an identical single-electron tunneling probability through the central molecule, the total transmission of the present OF device will be proportional to the efficient density of states (DOS) in the electrodes fallen into the bias window, $T_{\downarrow}(E) \propto D_{\downarrow \mathrm{L}}(E) \times D_{\downarrow \mathrm{R}}(E)$, where $D_{\downarrow \mathrm{L(R)}}(E)$ represents the DOS of the spin-down electrons with energy E in the left (right) electrode. $D_{\downarrow \mathrm{R}}(E)$ in the Au electrode is independent of the spin configurations, but it is known that $D_{\downarrow \mathrm{L}}(E)$ in the middle of the Co 3d band is much larger than that in the band edge.[41,42] As a result, the transmission in P configuration is much larger than that in AP configuration, which leads to a large TMR.

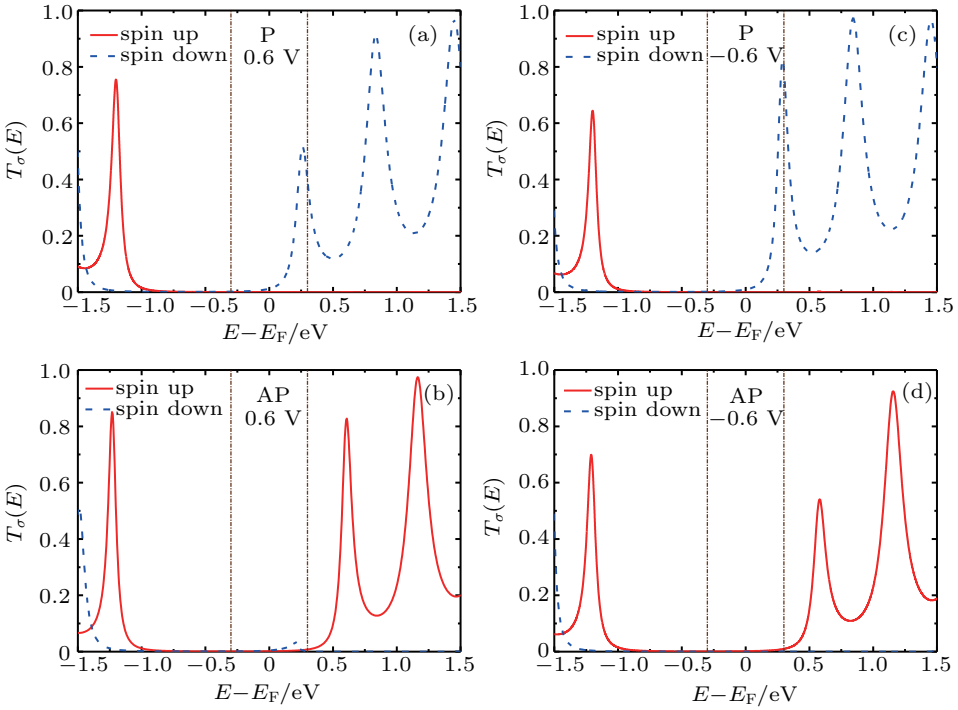


Fig. 3. The spin-dependent transmission spectra near the Fermi energy at different biases and spin configurations: (a), (b) P and AP configurations at 0.6 V; (c), (d) P and AP configurations at −0.6 V. The vertical dashed-dotted lines represent the conducting bias window.

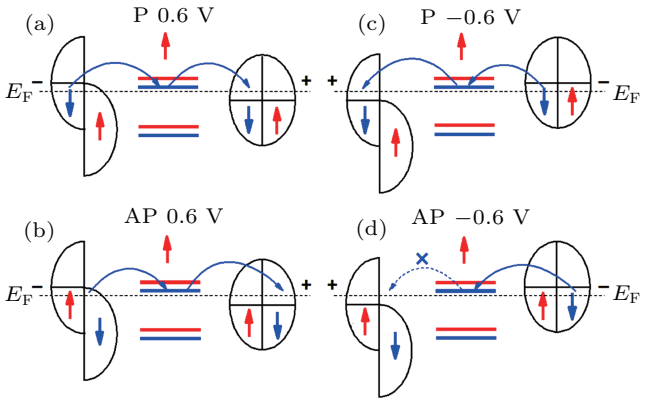


Fig. 4. The band tunneling sketch of the ferromagnet/OF/metal junction: (a) P configuration at 0.6 V, (b) AP configuration at 0.6 V, (c) P configuration at −0.6 V, (d) AP configuration at −0.6 V. Red (blue) upward (downward) arrows and lines stand for the spin-up (spin-down) magnetic moments and levels. Plus (minus) sign denotes the polarity of the bias.

With the reversal of the bias, the right Au band is lifted and the left Co band is lowered. In P configuration, the tunneling occurs between the middle of the two spin-down bands of the electrodes. Thus an efficient transmission still exists in the bias window similar to that in Fig. 4(a). However, in AP configuration, the tunneling of the spin-down electrons from Au to Co is forbidden due to the full-filled spin-down band in Co. As a result, the total transmission in AP configuration is completely suppressed, which is the source of the extremely high TMR at the negative bias.

It should be pointed out that besides the full-filled subband in Co, the OF adopted here plays a crucial role for the transport prohibition in AP configuration as well as the extremely large TMR, since it blocks the transmission of electrons with another spin. Such situation is hardly seen in the conventional organic spin valves with a ferromagnet/nonmagnetic-molecule/ferromagnet (FM/NM/FM) structure. The proposed OF spin valves are superior to conventional FM/NM/FM spin valves due to the spin selection of the central molecule, which will enlarge the difference of the efficient tunneling states between P and AP configurations, and then enhance the magnitude of the TMR. Such effect can be understood by the following analysis. For the FM/NM/FM structure, we assume that the electron DOS in the FM with different spins are D and d at the Fermi energy. In the limitation of low bias, the conductance in P configuration is usually contributed by both the majority and the minority electrons as $G_P \propto (D\times D + d\times d)$, while that in AP configuration reads $G_{AP} \propto (D\times d + d\times D)$. As a result, the TMR in the NM junction is $\mathrm{TMR}^{NM} = \frac{G_P - G_{AP}}{G_{AP}} \propto \frac{(D-d)^2}{2Dd}$. For the FM/OF/metal junction, due to the spin selection of the OF, only one of the majority and minority works, where the conductance is proportion to $D_0\times D$ and $D_0\times d$ in P and AP configurations, respectively. Here D_0 is the DOS of the tunneling electron in the right nonmagnetic metal. Thus the TMR is expressed as $\mathrm{TMR}^{FM} \propto \frac{D-d}{d} = \frac{(D-d)^2}{Dd-d^2}$. In the case of positive TMR ($D > d$), one obtains $2Dd > Dd - d^2$, which means that the TMR in the OF spin valve should be larger than that in the conventional FM/NM/FM one.

The above analysis can be further verified by the following additional numerical calculations for the FM/NM/FM and FM/OF/Au junctions with the same FM. Here the on-site energy of the FM is modified as $\varepsilon_l = -5.0$ eV to simulate a

more common situation where neither spin subbands are full-filled. These parameters generate a spin polarization of about 33% for the FM, which is close to Fe.[43] For the NM, the spin coupling strength j is set to zero. The other parameters are the same as above. As demonstrated in Fig. 5, the TMR in the FM/NM/FM junction is below 10%, which is consistent to experimental reports on organic spin valves with Fe electrode.[44] However, in the case of the Fe/OF/Au junction, the TMR is remarkably increased and a maximum value of about 90% is achieved at negative bias. We also examine the TMR in the Co/NM/Co junction, where the maximum TMR is only 1360% and much smaller than that in the Co/OF/Au junction.

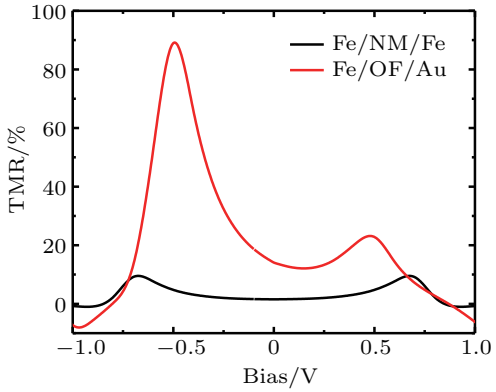


Fig. 5. Bias-dependent TMR in Fe/NM/Fe and Fe/OF/Au junctions.

The softness and spin correlation with radicals are crucial in determining the spin-dependent transport property of the OF device. The effects of the electron–lattice coupling (α) and the antiferromagnetic coupling with radicals (j) are discussed. The parameters of the Co/OF/Au junction are used. In Fig. 6, the TMR of the device is plotted with different values of α and j. As shown in Fig. 6(a), with the increase of j, a remarkable increase is observed for the TMR peaks, especially that at the negative bias. The maximum value reaches almost 5000% with $j = 0.6$. A little shift of the TMR peaks to the Fermi energy also occurs, which is due to the larger spin splitting of the molecular π orbitals with a larger j. In Fig. 6(b), one can find that with the increase of α, the TMR peaks are driven away from the Fermi energy, which is caused by the increased larger Peierls gap. An enhancement of the TMR peak at negative bias is also observed, which increases from about 3000% at $\alpha = 4.0$ to about 4000% at $\alpha = 4.4$. This indicates that within the involved strength, the electron–lattice coupling and spin correlation are helpful for enhancing the TMR. However, here we should comment that the above conclusion is obtained in the frame of SSH model, where the electron–lattice interaction mainly modulates the band gap and the electronic states, while possible phonon induced spin flipping process is not considered. It is also noticed that in several other reports, the TMR and current spin polarization were weakened in the presence of lattice vibration.[45,46] The difference is related to the involved specific materials, such as the band symmetry in graphene nanoribbons.

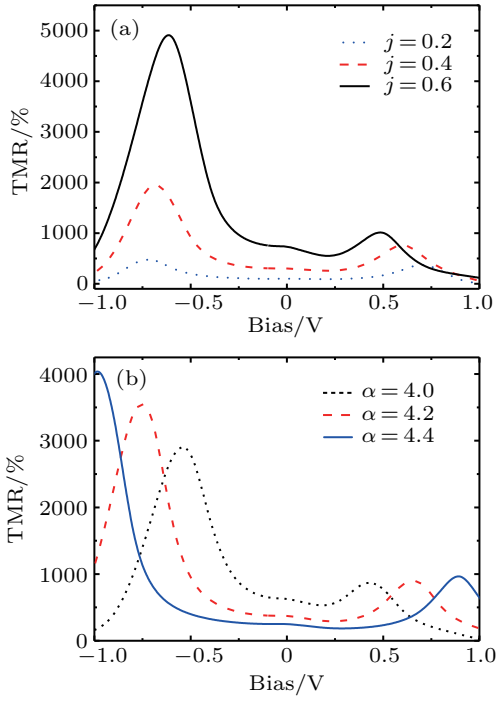


Fig. 6. Dependence of the TMR on (a) spin coupling parameter j and (b) electron–lattice coupling parameter α of the central OF.

At last, we further study the effect of the molecular length on the TMR. The results are displayed in Fig. 7. It is seen that the peaks of the TMR shift towards the Fermi level with the increase of the molecular length, which originates from the decrease of energy gap with the chain length. However, it is noticed that the maximum magnitude of the TMR increases with the length. For example, the TMR is about 500% at -1.0 V with $N = 12$, while it reaches about 7300% at -0.53 V with $N = 24$. A similar dependence of the TMR on molecular chain length has been reported in normal nonmagnetic polymer spin valves.[47]

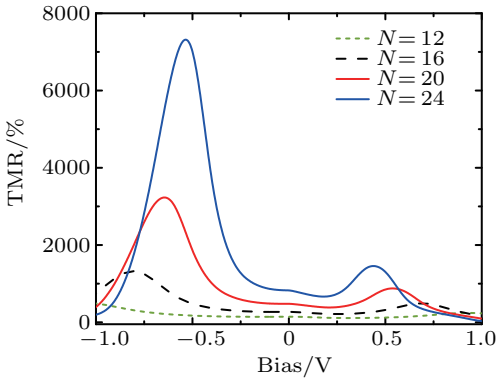


Fig. 7. Dependence of TMR on the length of the central OF.

4. Summary

In conclusion, the spin-dependent transport in a ferromagnet/OF/metal junction is investigated. The results demonstrate that by controlling the relative magnetization orientation of the ferromagnet and the central OF, a giant TMR up to 3230% is realized. The mechanism is explored in terms of transmission and band tunneling sketch, where the large TMR is explained by the asymmetric efficient tunneling states in the ferromagnet in P and AP configurations combined with the spin selection effect of the central OF. This work indicates that high-performance organic spin valves are expected with the utilization of the OFs, which deserve further verification in experiments. Moreover, the revealed physics gives us a hint to enhance the TMR in molecular spin valves, that is, generating a spin-filtering effect in the central region, which may be realized by using spin radicals or designing fully spin-polarized hybridized interfacial states. We also notice other similar reports where metallocene-dimers or magnetic ions doped carbon nanotube are adopted to enhance the TMR by adjusting the spin configurations of the central molecule,[48] and even a thermoelectric conversion effect is found where a pure spin current is generated.[49] Such effect deserves further investigation in present FM/OF/NM type devices.

References

[1] Dieny B, Speriosu V S, Parkin S S P, Gurney B A, Wilhoit D R and Mauri D 1991 *Phys. Rev. B* **43** 1297

[2] Park B G, Wunderlich J, Martí X, Holý V, Kurosaki Y, Yamada M, Yamamoto H, Nishide A, Hayakawa J, Takahashi H, Shick A B and Jungwirth T 2011 *Nat. Mater.* **10** 347

[3] Cai K M, Yang M Y, Ju H L, Wang S M, Ji Y, Li B H, Edmonds K W, Sheng Y, Zhang B, Zhang N, Liu S, Zheng H Z and Wang K Y 2017 *Nat. Mater.* **16** 712

[4] Sheng Y, Edmonds K W, Ma X Q, Zheng H Z and Wang K Y 2018 *Adv. Electron. Mater.* **4** 1800224

[5] Cao Y, Rushforth A W, Sheng Y, Zheng H Z and Wang K Y 2019 *Adv. Funct. Mater.* **29** 1808104

[6] Xiong Z H, Wu D, Vardeny Z V and Shi J 2004 *Nature* **427** 821

[7] Schoonus J J H M, Lumens P G E, Wagemans W, Kohlhepp J T, Bobbert P A, Swagten H J M and Koopmans B 2009 *Phys. Rev. Lett.* **103** 146601

[8] Santos T S, Lee J S, Migdal P, Lekshmi I C, Satpati B and Moodera J S 2007 *Phys. Rev. Lett.* **98** 016601

[9] Sun D, Yin L, Sun C, Guo H, Gai Z, Zhang X G, Ward T Z, Cheng Z and Shen J 2010 *Phys. Rev. Lett.* **104** 236602

[10] Devkota J, Geng R, Subedi R C and Nguyen T D 2016 *Adv. Funct. Mater.* **26** 3881

[11] Liu R, Bi J J, Xie Z, Yin K K, Wang D Y, Zhang G P, Xiang D, Wang C K and Li Z L 2018 *Phys. Rev. Appl.* **9** 054023

[12] Li Z L, Sun F, Bi J J, Liu R, Suo Y Q, Fu H Y, Zhang G P, Song Y Z, Wang D Y and Wang C K 2019 *Physica E* **106** 270

[13] Sun F, Liu R, Suo Y Q, Niu L L, Fu H Y, Ji W F and Li Z L 2019 *Acta. Phys. Sin.* **68** 178502 (in Chinese)

[14] Pramanik S, Stefanita C G, Patibandla S, Bandyopadhyay S, Garre K, Harth N and Cahay M 2007 *Nat. Nanotechnol.* **2** 216

[15] Sanvito S 2010 *Nat. Phys.* **6** 562

[16] Dediu V A, Hueso L E, Bergenti I and Taliani C 2009 *Nat. Mater.* **8** 707

[17] Barraud C, Seneor P, Mattana R, Fusil S, Bouzehouane K, Deranlot C, Graziosi P, Hueso L, Bergenti I, Dediu V, Petroff F and Fert A 2010 *Nat. Phys.* **6** 615

[18] Yue F J, Shi Y J, Chen B B, Ding H F, Zhang F M and Wu D 2012 *Appl. Phys. Lett.* **101** 022416

[19] Yu C J, Miao Y Y, Qiu S, Cui Y J, He G M, Zhang G P, Wang C K and Hu G C 2018 *J. Phys. D: Appl. Phys.* **51** 345302

[20] Yoo J W, Edelstein R S, Lincoln D M, Raju N P, Xia C, Pokhodnya K I, Miller J S and Epstein A J 2006 *Phys. Rev. Lett.* **97** 247205

[21] Fang Z, Liu Z L and Yao K L 1994 *Phys. Rev. B* **49** 3916

[22] Fang Z, Liu Z L, Yao K L and Li Z G 1995 *Phys. Rev. B* **51** 1304

[23] Yoo J W, Chen C Y, Jang H W, Bark C W, Prigodin V N, Eom C B and Epstein A J 2010 *Nat. Mater.* **9** 638

[24] Li B, Zhou M Q, Lu Y, Kao C Y, Yoo J W, Prigodin V N and Epstein A J 2012 *Org. Electron.* **13** 1261

[25] Hayakawa R, Karimi M A, Wolf J, Huhn T, Zöllner M S, Herrmann C and Scheer E 2016 *Nano Lett.* **16** 4960

[26] Hu G C, Guo Y, Wei J H and Xie S J 2007 *Phys. Rev. B* **75** 165321

[27] Wang W Z 2006 *Phys. Rev. B* **73** 235325

[28] Hu G C, Zhang Z, Zhang G P, Ren J F and Wang C K 2016 *Org. Electron.* **37** 485

[29] Hu G C, Zuo M Y, Li Y, Ren J F and Xie S J 2014 *Appl. Phys. Lett.* **104** 033302

[30] Ovchinnikov A A and Spector V N 1988 *Synth. Met.* **27** 615

[31] Alberola A and Pilkington M 2009 *Curr. Org. Synth.* **6** 66

[32] Su W P, Schrieffer J R and Heeger A J 1979 *Phys. Rev. Lett.* **42** 1698

[33] Shuai Z, Pati S K, Su W P, Brédas J L and Ramasesha S 1997 *Phys. Rev. B* **55** 15368

[34] Xie S J, Ahn K H, Smith D L, Bishop A R and Saxena A 2003 *Phys. Rev. B* **67** 125202

[35] Mujica V, Roitberg A E and Ratner M 2000 *J. Chem. Phys.* **112** 6834

[36] Datta S 1995 *Electronic Transport in Mesoscopic Systems* (New York: Oxford University Press) p. 92

[37] Miao Y Y, Qiu S, Zhang G P, Ren J F, Wang C K and Hu G C 2018 *Org. Electron.* **55** 133

[38] Miao Y Y, Qiu S, Zhang G P, Ren J F, Wang C K and Hu G C 2018 *Phys. Rev. B* **98** 235415

[39] Aschcroft N W and Mermin N D 1976 *Solid State Physics* (Philadelphia: Saunders College) p. 290

[40] Cao Y, Wang P, Hu Z Y, Li S Z, Zhang L Y and Zhao J G 1988 *Synth. Met.* **27** 625

[41] Botton G A, Guo G Y, Temmerman W M and Humphreys C J 1996 *Phys. Rev. B* **54** 1682

[42] He G M, Qiu S, Cui Y J, Yu C J, Miao Y Y, Zhang G P, Ren J F, Wang C K and Hu G C 2019 *J. Mater. Sci.* **54** 5551

[43] Park C H, Lee B C and Lee J I 2005 *J. Korean. Phys. Soc.* **47** 655

[44] Wang F J, Xiong Z H, Wu D, Shi J and Vardeny Z V 2005 *Synth. Met.* **155** 172

[45] Liu Y Y, Li B L, Chen S Z, Jiang X W and Chen K Q 2017 *Appl. Phys. Lett.* **111** 133107

[46] Li B L and Chen K Q 2016 *J. Phys.: Condens. Matter* **29** 075301

[47] Wei J H, Xie S J, Mei L M, Berakdar J and Yan Y J 2007 *Org. Electron.* **8** 487

[48] Zeng J and Chen K Q 2014 *Appl. Phys. Lett.* **104** 033104

[49] Wu D, Cao X H, Chen S Z, Tang L M, Feng Y X, Chen K Q and Zhou W X 2019 *J. Mater. Chem. A* **7** 19037